Jpn. J. Vet. Res. 50(2 - 3) : 125-139, 2002

FULL PAPER

Cellular architecture of the synovium in the tendon sheath of horses : An immunohistochemical and scanning electron microscopic study

Morimasa Kohama, Junko Nio, Yoshiharu Hashimoto and Toshihiko Iwanaga*

(Accepted for publication : November 5, 2002)

Abstract

The intimal lining cells of the synovium in joints have been studied morphologically and histochemically and shown to consist of macrophagic cells (type A) and fibroblast-like cells (type B). It is believed that the structure of the synovium in the tendon sheath is similar to that in the joint, but there have been only a few morphological studies of the tendon sheath. The present study revealed the cellular architecture of synovium in the tendon sheath of horses by histochemistry and scanning electron microscopy (SEM). Like the joint, the inner surface of the tendon sheath was covered with a cell-rich intimal layer. Acid phosphatase-positive A cells accumulated in the mesotendon but few in other regions. B cells were selectively immunolabeled with protein gene product (PGP) 9.5 antiserum and distributed in the entire length of the synovial intima in the tendon sheath. The synovial intima consisted of a surface layer rich in the processes of B cells and a deep layer containing cell bodies of B cells. Using SEM, B cells could be classified into two types according to the morphology of their processes. B cells of dendritic type were located mainly in the joint-side of the tendon sheath and extended branched processes to form a meshwork on the intimal surface. B cells of flat type were located in the skin-side of the tendon sheath and in the mesotendon. Their membranous processes extended in a horizontal direction and covered the intimal surface, resembling epithelium. It appears likely that the morphology and distribution of synovial intimal cells are influenced by various factors, such as the nature of the underlying tissues and the magnitude of mechanical stress.

Laboratory of Anatomy, Department of Biomedical Sciences, Graduate School of Veterinary Medicine, Hokkaido University, Sappro 060-0818, Japan

*Corresponding author : Toshihiko Iwanaga, Laboratory of Anatomy, Graduate School of Veterinary Medicine, Hokkaido University, Kita 18-Nishi 9, Kita-ku, Sapporo 060-0818, Japan

TEL : +81-11-706-5187

FAX : +81-11-706-5190

Key words : tendon sheath ; synovium ; scanning electron microscopy ; PGP 9.5 ; horse

Introduction

The synovium (or the synovial membrane) of joints is covered with the synovial intima, which is the innermost cell-rich layer and is composed of macrophage-derived type A cells and fibroblast-like type B cells[3,11,12,20,29]. A cells are abundant in the synovial villi and folds, and are basically exposed to the joint cavity. They function in the homeostasis of the joint cavity by phagocytosing wastes and cell debris in the synovial fluid[2,13,17,33,34,37]. Fibroblast-like B cells are cells specific to the synovium and are characterized by branched cytoplasmic processes which extend toward the joint cavity. B cells possess developed rough endoplasmic reticulum in their cytoplasm, and secrete intercellular matrix or components of synovial fluid, including collagen, fibronectin, and hyaluronic acid[9,22,23,24,30,31,32,43]. Many histochemical methods have been used for detecting each type of synovial intimal cell[15]. A cells can easily be labeled immunohistochemically using antibodies against macrophages or by enzyme-histochemical staining for acid phosphatase, which is one of the major lysosomal enzymes. B cells have been detected with immuno- or enzyme-histochemistry using enzymes for collagen- and hyaluronan-synthesis, vascular cell adhesion molecule-1 (VCAM-1) and heat shock protein 25 as markers. We found that in the horse, synovial B cells react with antibodies against protein gene product (PGP) 9.5, and we showed the usefulness of PGP9.5 as a cytochemical marker of B cells[19].

Although scanning electron microscopy (SEM) is useful for analyzing the three-dimensional ultrastructure of cells, it is difficult to observe the whole shape of a given synovial intimal cell because these cells are embedded in abundant intercellular matrix. Many SEM observations of synovial intimal cells have failed to reveal the entire image clearly[7,8,25,41,42], but this problem was solved by removing the intercellular matrix using the NaOH maceration method[35].

The synovium exists not only in the joint cavity but also in the tendon sheath and the synovial bursa. Morphological studies on the synovium of the tendon sheath have been carried out in various species (rats, rabbits, goats, dogs, horses, humans), and it is believed that its structure is similar to that of the joint[1,6,16,18,21,28,36,38,40]. However, information on the morphology of synovial intimal cells in the tendon sheath is lacking, and previous ultrastructural studies using transmission electron microscopy (TEM) or conventional SEM revealed only portions of cells.

In the present study we examined the distribution and three-dimensional ultrastructure of synovial intimal cells in the tendon sheath of horses by histochemistry and by SEM using NaOH-macerated samples.

Materials and Methods

Animals and tissue sampling

Five thoroughbred horses ranging in age from 10 to 22 years without any abnormalities in the joint or tendon sheath were used in this study. All experiments were performed using protocols following the Guidelines for Animal Experimentation, Graduate School of Veterinary Medicine, Hokkaido University. The animals were deeply anesthetized with pentobarbital and thiopental sodium and were sacrificed by bloodletting from the cervical artery. The tendon sheaths of the common digital extensor on both sides were quickly removed

and fixed in 4 % paraformaldehyde in 0.1M phosphate buffer (PB, pH 7.4) overnight at 4℃ for light microscopic observation. Tissue samples were also fixed in 2 % glutaraldehyde in 0.1M PB overnight at 4℃ for SEM observation. The paraformaldehyde-fixed tissues were transected into small pieces and dipped in 30% sucrose solution overnight at 4℃. Frozen sections about 10μm thick were prepared using a cryostat (CM 3050 ; Leica, Nussloch, Germany) and mounted on poly-L-lysine-coated glass slides. The sections were used for hematoxylin and eosin (H-E) staining, immunostaining for PGP 9.5 and enzyme histochemistry for acid phosphatase.

Immunohistochemistry for PGP 9.5

Immunostaining of PGP 9.5 was carried out according to the avidin-biotin complex (ABC) method. The sections were treated with 0.3% Triton X-100 in 0.1M PBS (pH 7.4) for 1 hr and then with 0.3% H_2O_2 in methanol for inhibition of endogenous peroxidase activity. After treatment with a blocking serum for 30 min, the sections were incubated with various dilutions (from 10,000 to 15,000) of a rabbit polyclonal antiserum against human PGP 9.5 (RA 95101 ; Ultraclone, Isle of Wight, UK) overnight at room temperature. The sections were then incubated with biotinylated goat anti-rabbit immunoglobulin and avidin-peroxidase (Histofine kit ; Nichirei, Tokyo, Japan). The antigen-antibody reaction was visualized by incubation in 0.05M Tris-HCl buffer (pH 7.6) containing 0.01% 3,3'-diaminobenzidine (DAB) and 0.002% H_2O_2. The DAB reaction was enhanced by adding 0.04% nickel ammonium sulfate.

Acid phosphatase staining

For detection of acid phosphatase activity, frozen sections were stained according to Burnstone (1958). Control experiments for the acid phosphatase reaction were simultaneously carried out by incubating with medium containing 10mM NaF, a potent inhibitor of this enzyme. The activity was completely inhibited by preincubation of the medium with NaF.

Scanning electron microscopy (SEM)

The glutaraldehyde-fixed tissues were dissected into small pieces (3 × 3 × 3 mm) and processed according to the NaOH maceration method before conductive staining[39]. The fixed specimens were rinsed in 0.1M PB and subsequently placed in 6N NaOH at 60℃ for 15 to 60 min. After the alkaline maceration, the tissue blocks were degraded into small fragments by rigorous ejection through a fine pipette via a stream of 0.01M PB (pH 7.2). The specimens were then conductive-stained by the tannin-osmium method[26], and dehydrated through a graded series of ethanol. The tissue pieces were dipped in isoamyl acetate and critical point-dried using liquid carbon dioxide. The dried specimens were evaporation-coated with platinum-palladium and examined under a scanning electron microscope (S-4100 ; Hitachi, Tokyo, Japan).

Results

The synovium (synovial membrane) of the tendon sheath is divided into two membranous layers : the visceral layer which directly envelopes the tendon, and the parietal layer which is contralateral to the visceral layer via the tendon-sheath cavity. These two layers are joined by the mesotendon[10]. In this paper, the tendon sheath was considered to be divided into the following four regions (R) for description : the mesotendon (R1), the joint-side (R2), the side contralateral to the mesotendon (R3), and the skin-side (R4), as shown in Fig. 1A.

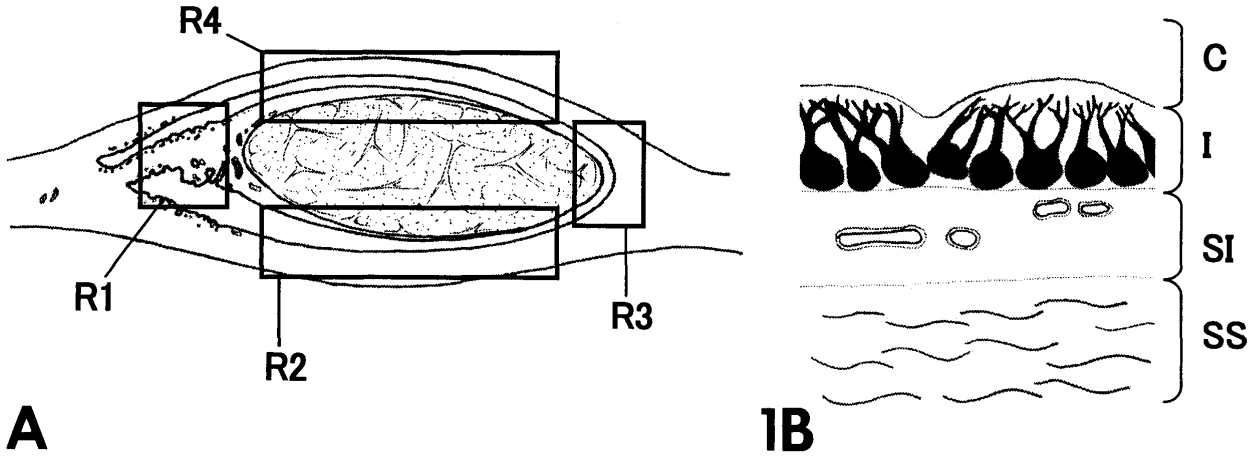

Fig. 1. Schematic diagram showing an overview of the tendon sheath (A) and the structure of the synovium (B). A. In this report, the tendon sheath was considered to be divided into the following four regions (R) : the mesotendon (R 1), the joint-side (R 2), the side contralateral to the mesotendon (R 3), and the skin-side (R 4). B. The interior of the tendon sheath cavity (C) is covered with a cell-rich layer, the synovial intima (I). The subintima (SI) is occupied by loose connective tissue containing abundant blood vessels (vascular layer). The subsynovium (SS) is densely arranged collagen tissue underlying the synovium.

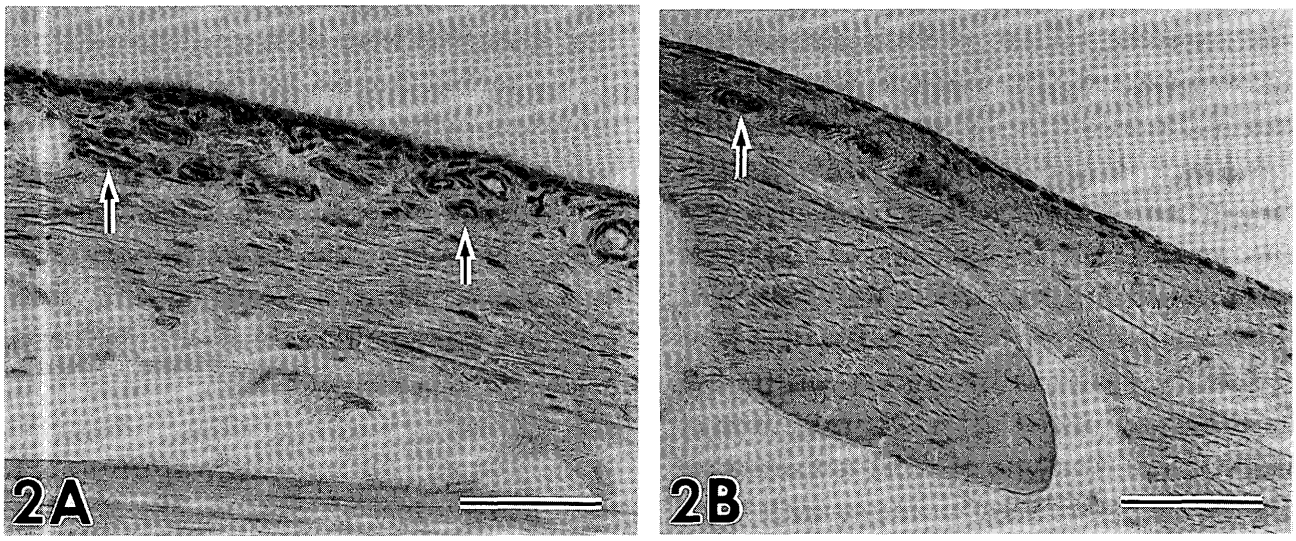

Fig. 2. Light microscopic observation of the parietal layer (A) and visceral layer (B) stained with hematoxylin-eosin. The subintimal vascular layer develops in the parietal layer, whereas it is scanty in the visceral layer. Arrows indicate blood vessels. Bars = 100 μm

Observation by light microscopy

Like the joint, the interior of the tendon sheath cavity was covered with a cell-rich layer, synovial intima (Fig. 1 B). The underlying tissue of the intima, termed the subintima, was occupied by connective tissue containing blood vessels. The underlying tissue of the subintima, termed the subsynovium, consisted of dense collagen fibers.

Light microscopic observation of the transversely cut tendon-sheath revealed the formation of folds or villi at the intima of the mesotendon (R 1) (Fig. 4). The intima of the parietal layer on the joint-side (R 2 and R 3) was thick, and more-or-less undulated (Figs. 3 A, B), while on the skin-side (R 4),

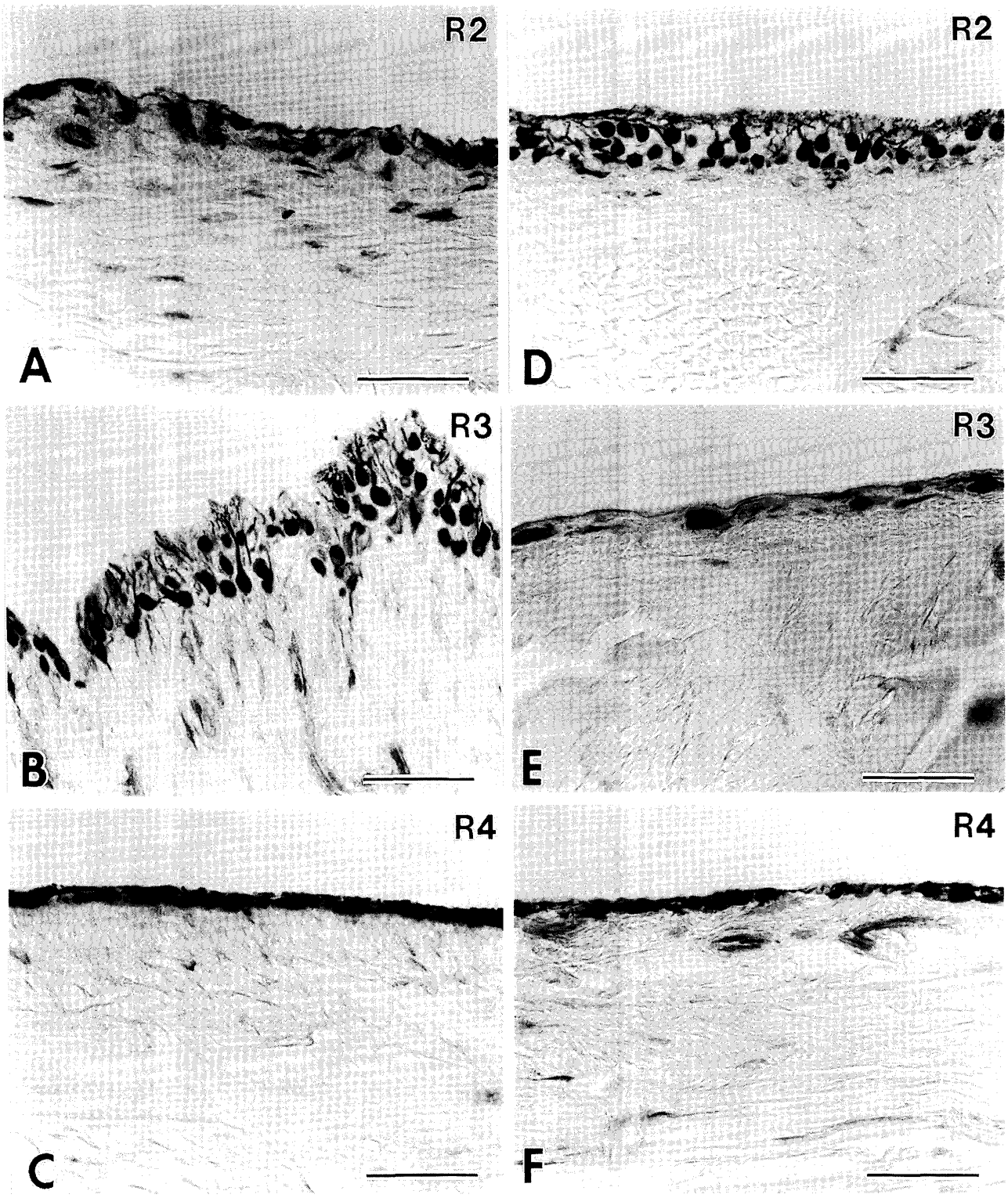

Fig. 3. Immunostaining of B cells in three different regions of the parietal (A-C) and visceral layers (D-F) by use of an anti-PGP 9.5 serum. The intima of the parietal layer in R 2 (A) and R 3 (B) is thick and more or less undulated, while in R4, it tends to be thin and smooth (C). PGP 9.5-positive B cells extend processes toward the tendon-sheath cavity, especially clearly in R 3 of the parietal layer (B) and R 2 of the visceral layer (D). In the visceral layer (D-F), the intima is smooth along the entire length. The intimal thickness of R 2 (D) and R 4 (F) shows the same tendency as that described above in the parietal layer. In R 3 of the visceral layer (E), the synovial intima is much thinner, and the distribution density of B cells is lowest. Bars=50μm

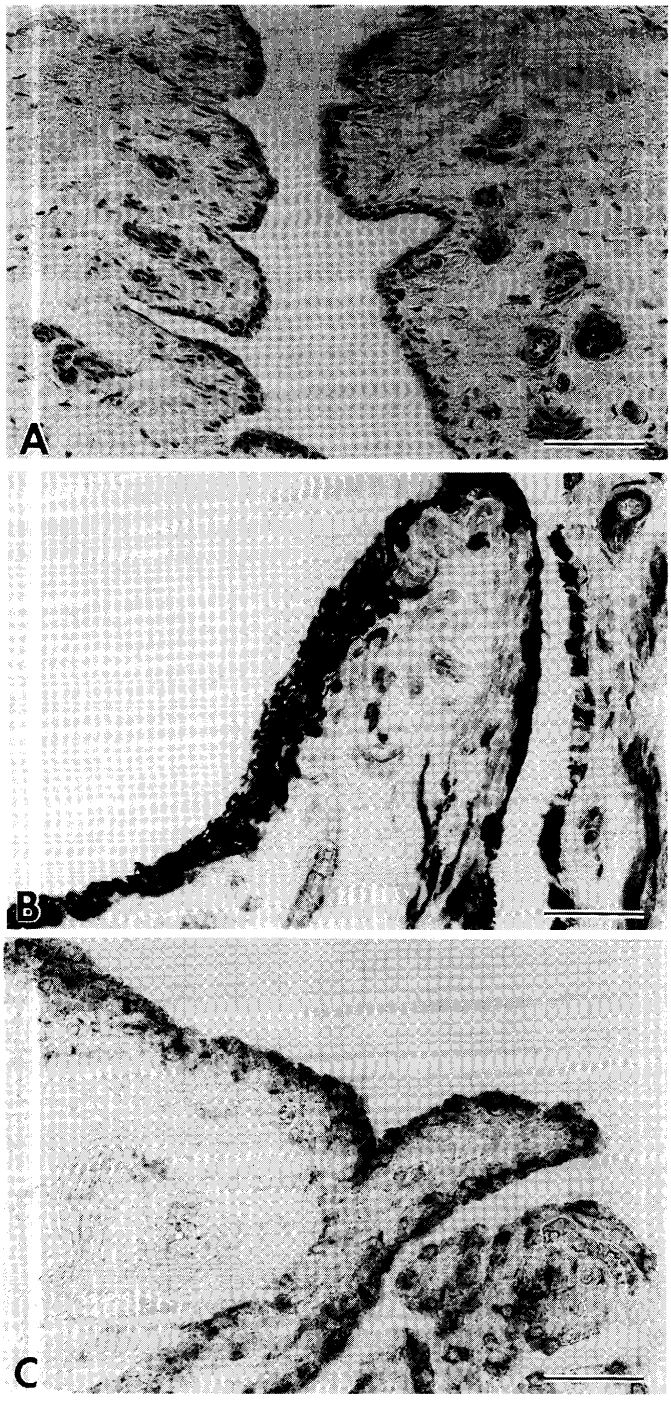

Fig. 4. Light microscopic observation of the mesotendon (R 1). H-E staining (A), immunostaining for PGP 9.5 (B) and acid phosphatase staining (C). The subintima is very thick loose connective tissue with developed blood vessels (A). The intima shows remarkable undulations, often displaying villi. Acid phosphatase-positive A cells accumulate in the mesotendon (C). Bars=100 μm (A), 50 μm (B, C)

it tended to be thin and smooth (Fig. 3 C). The synovial intima of the visceral layer was smooth along the entire length and showed the same tendency of thickness as that in the parietal layer (Figs. 3 D, F), except in R3, where it was much thinner (Fig. 3 E). The subintima of the parietal layer consisted of well-vascularized connective tissue, while in the visceral layer a scanty subintima intervened between the intima and the subsynovium (Figs. 2 A, B). The subintima of mesotendon (R 1) was occupied by areolar tissue with developed blood vessels (Fig. 4 A).

Immunohistochemistry for PGP 9.5 and histochemistry for acid phosphatase specifically detected B cells and A cells, respectively,

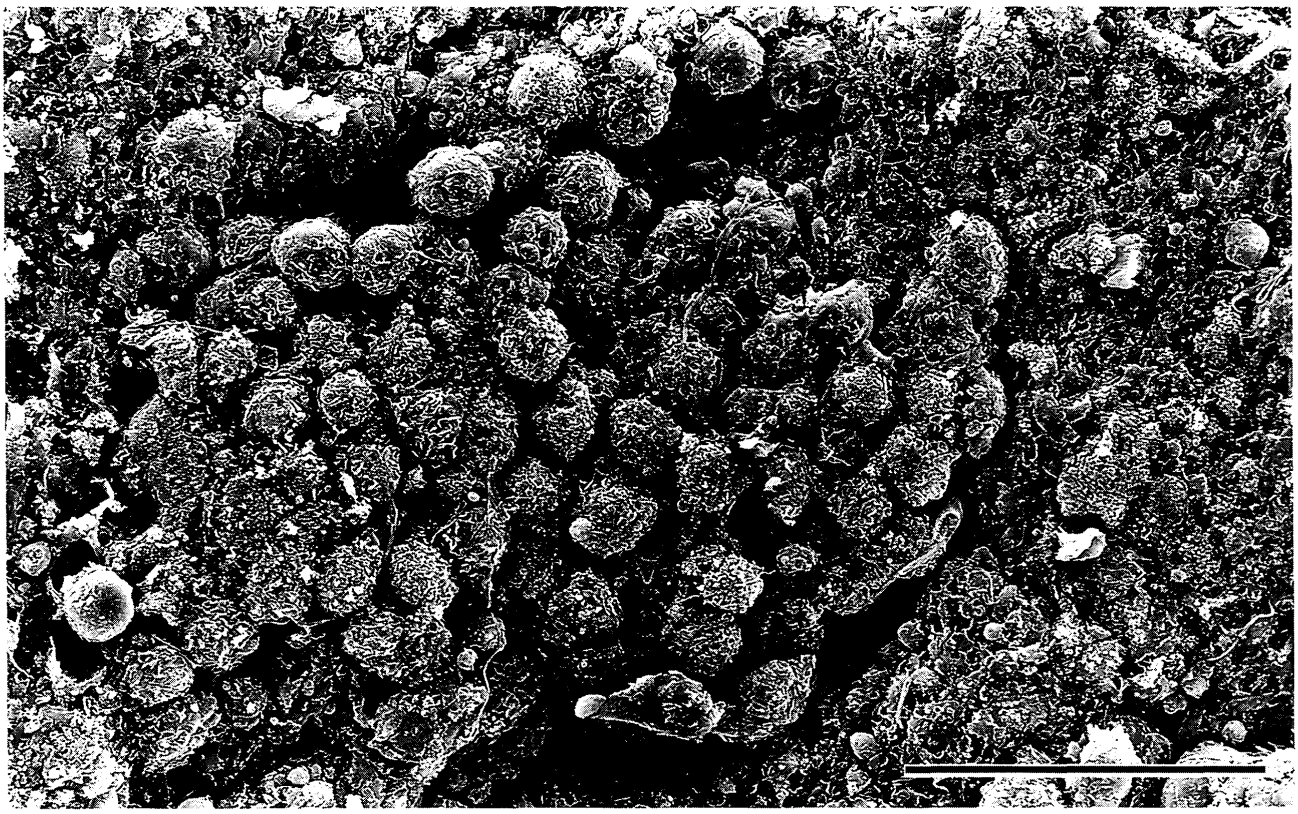

Fig. 5. A SEM image of conventional tissue sample in the mesotendon (R 1). Numerous A cells exposed on the intimal surface are visible, but the cell bodies and processes of B cells can not be observed because they are thoroughly embedded in the intercellular matrix. Bar=50 μm

and showed that B cells were distributed along the entire length of the tendon-sheath intima, and A cells accumulated in the mesotendon (R 1) (Fig. 4 C). The distribution density of all intimal cells was highest in the mesotendon (R 1) (Fig. 4) and lowest in R 3 of the visceral layer (Fig. 3 E). PGP 9.5 -positive B cells extended dendritic processes to form a thick layer of processes on the intimal surface, which was especially clear in R 3 of the parietal layer, R 2 of the visceral layer and the mesotendon (R 1), where their intima was thick (Figs. 3 B, D, 4 B).

Observation by scanning electron microscopy

In SEM observation of conventional tissue samples, A cells exposed on the intimal surface were visible, but the cell bodies and processes of B cells could not be observed because they were thoroughly embedded in the intercellular matrix (Fig. 5). Upon removal of the intercellular matrix by NaOH treatment, the cellular architecture of B cells with complicated processes was disclosed in all regions.

B cells could be classified into two types according to the morphology of their processes. B cells of the dendritic type (Fig. 6 D) were located mainly in the joint-side of the tendon sheath (R 2 and R 3), where the intima was thick. Their processes extended from deeply located cell bodies toward the tendon-sheath cavity, and formed a meshwork of processes on the intimal surface (Fig. 6 A). In the layer of processes, minute and irregular-shaped spaces appeared among the processes (Fig. 6 B), and it was shown by comparison with conventional samples that the layer of processes was wholly embedded with intercellular matrix or collagen fibers. One exception was that

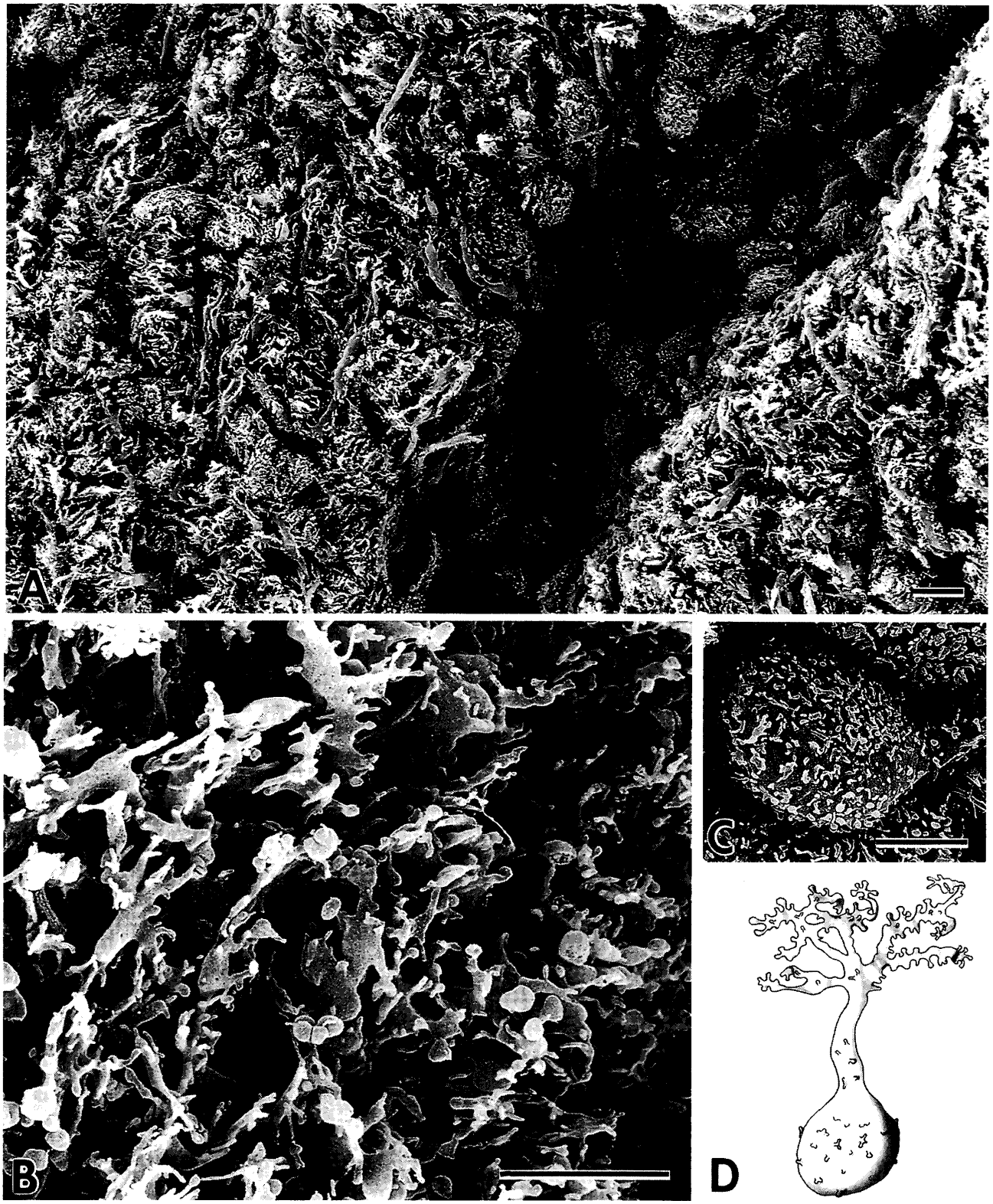

Fig. 6. SEM images of dendritic type of B cells in the parietal layer of R 2 (A, B, C) and schematic drawing of a typical cell (D). The dendritic-type B cells extend their processes from deeply located cell bodies toward the tendon-sheath cavity, and form a meshwork of processes on the intimal surface (A). Higher magnification of dendritic-type B cells shows terminal arborization of the processes (B). Dendritic-type B cells possess many microprotrusions on their surface (B, C). Bars=10 μm (A), 5 μm (B, C)

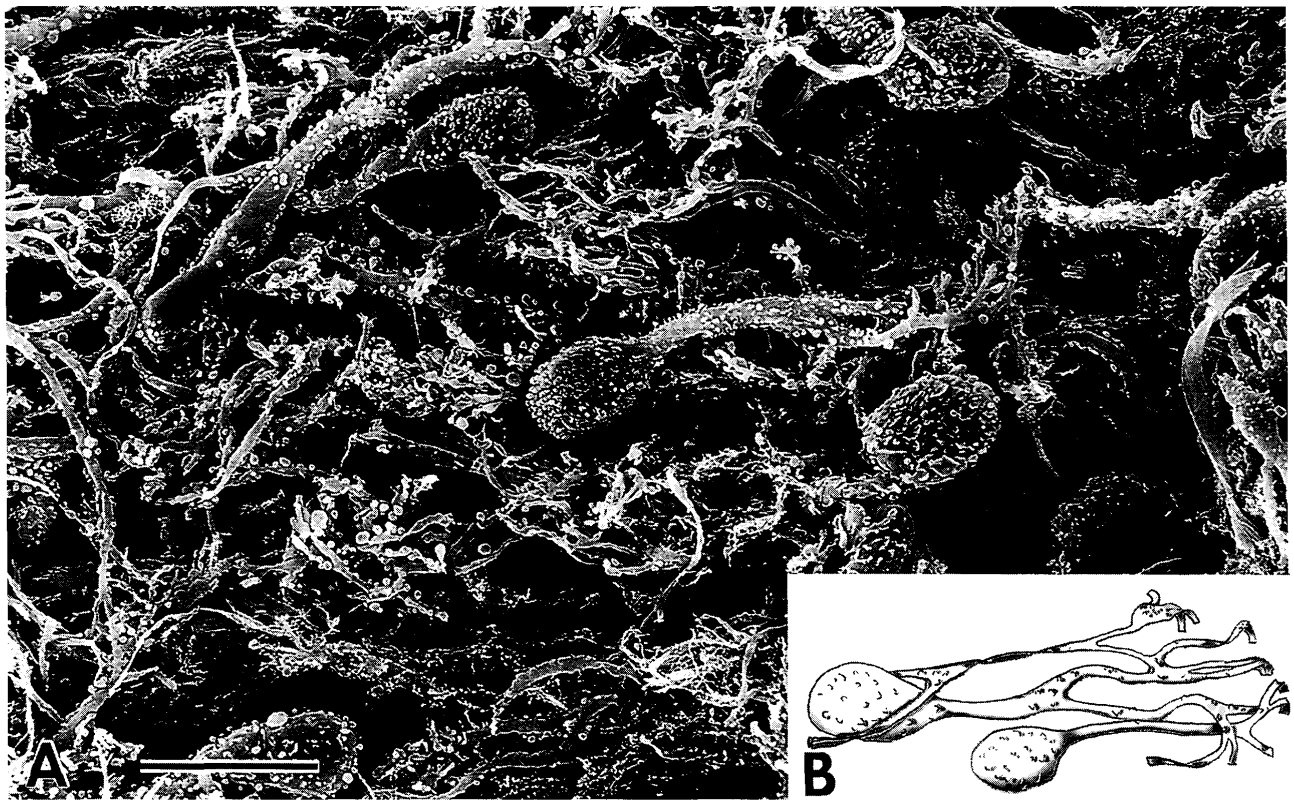

Fig. 7. An SEM image of the visceral layer of R 3 (A) and the schematic diagram of a dendritic-type B cell in this region (B). The processes of B cells extend in the horizontal direction. Bar=20 μm (A)

processes of B cells extended in a horizontal direction in the visceral layer of R 3, where the intima was thin, and it was impossible to distinguish between the cell body layer and process layer (Fig. 7A). The cell bodies and processes of dendritic-type B cells were also characterized by possessing many granular microprotrusions on their surface (Figs. 6 B, C).

B cells of the flat type (Fig. 8 D) were located in the mesotendon (R 1) and skin-side (R 4). Their processes were essentially flat, but varied from a wide leaf-form to a slender belt-form. They extended in the horizontal direction and covered the intimal surface (Figs. 8 A, B). In the skin-side (R 4), where the intima was thin, cell bodies of B cells tended to gather just under the surface layer of processes (Fig. 8 C). In the mesotendon (R 1) with a thick intima, flat-type B cells projected membranous processes that ultimately formed a thick process layer, which covered the cell bodies of B cells like epithelium (Fig. 9). These flat-type B cells possessed a few acicular microprotrusions (Fig. 8 C).

Discussion

The present study showed that fibroblast-like B cells were distributed widely in the intima of the tendon sheath, as they are in the joint synovium, in horses, and that they were selectively immunoreactive for PGP 9.5. The cell bodies of the B cells were located in a deeper layer of the intima and extended processes toward the tendon-sheath cavity. The processes branched delicately and formed a layer of processes on the intimal surface. The shape of these B cells was essentially similar to those of the B cells in the joint synovium[35], but their density and morphology were differ-

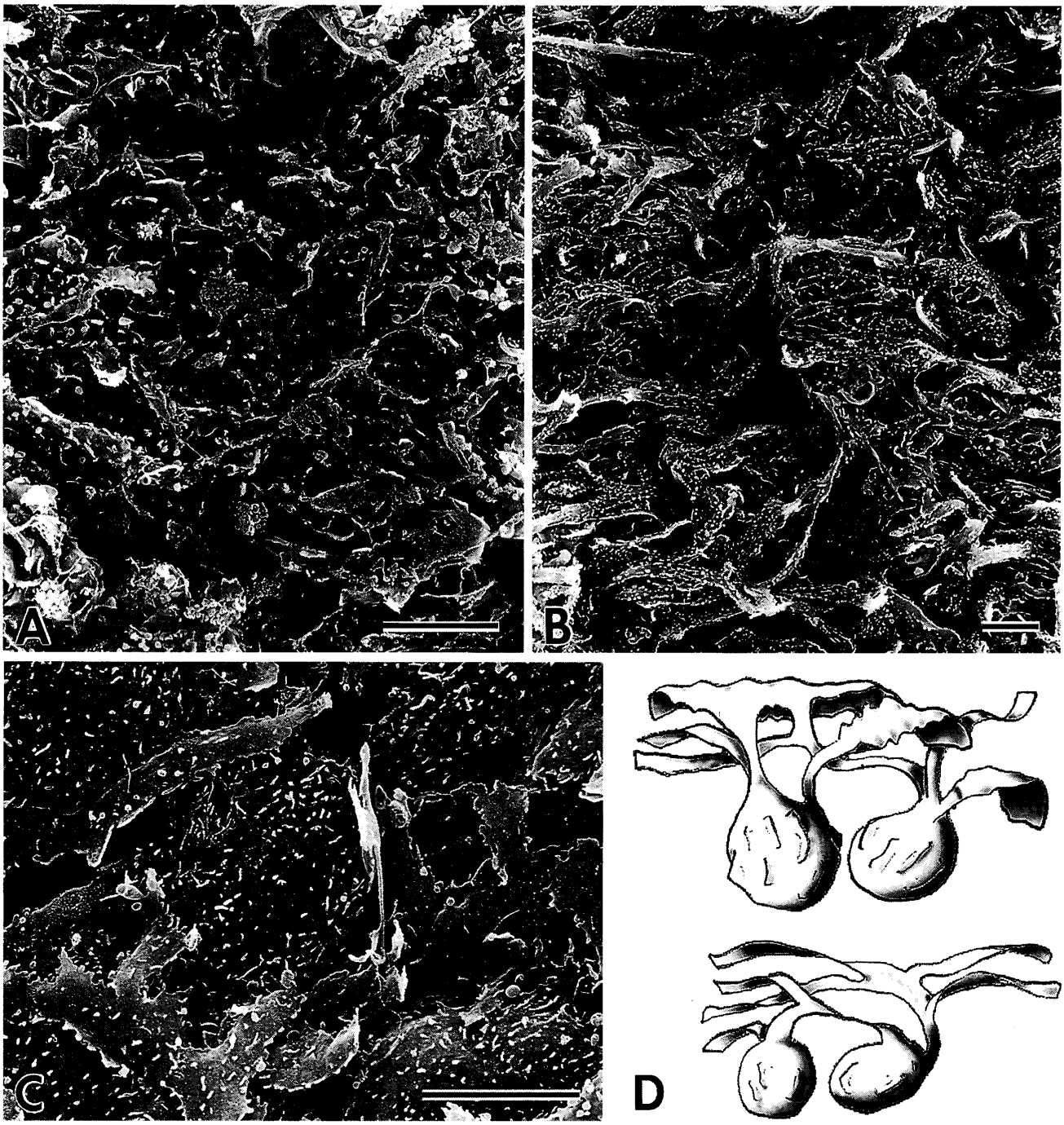

Fig. 8. SEM images of flat-type B cells (A, B, C) and a schematic diagram of typical flat-type B cells (D). The processes of flat-type B cells cover the intimal surface and vary from a wide leaf-form (A) to a slender belt-form (B). Flat-type B cells possess a few acicular microprotrusions on the cell bodies and processes (C). Bars=10 μm (A-C)

ent. On the other hand, acid phosphatase-positive A cells accumulated in the mesotendon and were very rare in other regions.

The morphology of the synovial intima in the parietal and visceral layers

The synovial intima of the parietal layer in the skin-side was thin and smooth, while that in the joint-side was thick and undulated. The subintimal vascular layer was also more

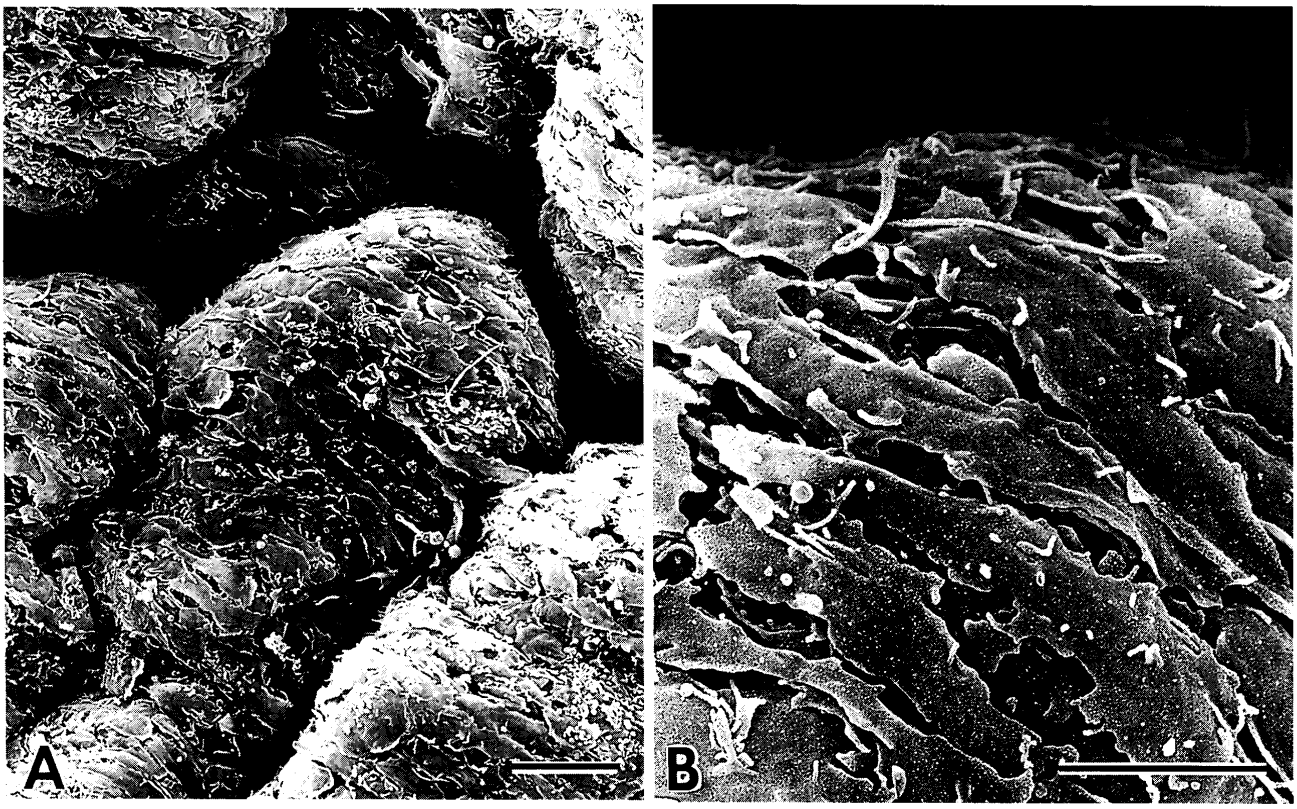

Fig. 9. SEM images of the mesotendon (R 1). Membranous processes of flat-type B cells cover the synovial intima, resembling epithelium, and cell bodies of B cells are completely embedded. Bars=10 μm (A), 5 μm (B)

developed in the joint-side. Hago et al. (1990) reported briefly that intimal undulations were seen in the parietal layer of the tendon-sheath synovium in the horse, but in the present study the undulations were observed only in the joint-side of the parietal layer. Since the subsynovial collagenous tissue supporting the parietal layer of the joint-side also serves as the joint-cavity wall, the parietal layer expands and contracts with the movement of the joint. It is convenient to think of the surface undulations of the intima as "wrinkles" whose formation is accompanied by the stretching movement, and that the development of the vascular layer in the joint-side confers flexibility on the joint. On the other hand, in the skin-side where the intimal surface is flat and smooth, the frictional resistance toward the tendon may be smaller than that in the joint-side intima.

A previous study using the tendon sheath of horses showed that B cells were hardly seen except in the mesotendon area[14]. In contrast, the present observation demonstrated a nearly constant distribution of B cells in all of the regions of the tendon-sheath intima. We were able to classify B cells into two types based on the morphology of their processes in both the parietal and visceral layers. In the joint-side, they were dendritic in shape, and projected complicated branched processes. It is considered that the fine meshwork of processes contributes to the anchoring of the abundant intercellular matrix in the intimal layer. Furthermore, the sponge-like structure ultimately formed by the processes may contribute to shock absorption during stretching movements. The cell bodies and processes of

dendritic-type B cells possess many granular microprotrusions on the surface. Although the functional significance of the microprotrusions is unknown, they may be related to some active secretory function of B cells[22,35].

Flat-type B cells were predominant in the skin-side where the intima was thin and smooth. Their membranous processes showed a lamellar arrangement and covered the intimal surface. In the joint synovium of rabbits, flat-type B cells are numerous in the regions adhering to the femur, where friction and pressure are relatively great, while dendritic-type B cells are predominant in the other regions[29]. Therefore, the morphology of flat-type B cells might reflect frictional resistance and resistance to compression.

The morphology of synovial intima in mesotendon

The mesotendon is abundant in blood vessels, because blood vessels pass through the mesotendon to enter the tendon. The accumulation of A cells in the mesotendon is in agreement with the fact that A cells are derived from monocytes in blood[27]. The rich supply of blood in the mesotendon suggests that the mesotendon is an important region for the production of synovial fluid. On the other hand, the mesotendon receives strong mechanical stress due to the movement of the tendon. Actually, the synovial intima in the mesotendon showed remarkable undulations, often displaying villi. Judging from the structure of the mesotendon and the magnitude of mechanical stress there, it might have been predicted that B cells in the mesotendon would be of the dendritic type, like those in the joint-side, but instead they were actually flat-type B cells.

The synovial fluid is mainly derived from blood, but its protein composition is considerably different from that of blood[5]. It has been considered that the processes of B cells and/or the intercellular matrix in the intima constitute a barrier between blood and synovial fluid (blood-joint barriar)[3,35]. The mesotendon, which is abundant in blood, is the major region secreting the components of synovial fluid. The presence of numerous flat-type B cells with membranous processes may be related to barrier functions against transport and secretion to the tendon-sheath cavity.

Conclusion

Many SEM observations of the joint synovium have indicated that the morphology of B cells varies according to their place in the joint. It is believed that the morphology of synovial intimal cells is affected by the nature of the underlying tissue, the development of vessels, and the magnitude of local movement. The present study of tendon-sheath synovium revealed different densities and morphologies of intimal cells, and could show a relation between the diversity of intimal cells and the external factors mentioned above. However, the shape of B cells was not uniform in the visceral layer, whose underlying tissue was collagenous tissue along the entire length. Moreover, the morphology of B cells was different between the mesotendon and the parietal layer of the joint-side, which both two regions receive great mechanical stress. These findings may indicate that the morphologic features of B cells reflect not only external factors but also their functions in loco.

In the present study, we used the tendon sheath from horses over 10 years of age. Hago et al. (1990), who observed tendon sheaths of young horses, reported that the processes of B cells extended in parallel along the tendon. Furthermore, the tissue samples we observed were tendon sheath of the common digital extenser, and our observations were restricted to a central part located on the carpal articu-

lar. It can probably be assumed that the morphology of synovial intimal cells in the central part differs from those in distal or proximal parts of the tendon sheath. More extensive examination of the age differences and regional differences of the morphology of synovial intimal cells are needed.

Acknowledgements

The authors thank Dr. Masahiro Okumura, Laboratory of Veterinary Surgery, for cooperation with the sampling.

References

1) Andreyev, P. P. 1948. On the structure of joints in the horse. *Veterinariya*, 25 : 20-25.
2) Ball, J., Chapman, J. A. and Muirden, K. D. 1964. The uptake of iron in rabbit synovial tissue following intraarticular injection of iron dextran. A light and electron microscope study. *J. Cell Biol.*, 22 : 351-364.
3) Barland, P., Novikoff, A. B. and Hamermen D. 1962. Electron microscopy of the human synovial membrane. *J. Cell Biol.*, 14 : 207-222.
4) Burnstone, M. S. 1958. Histochemical demonstration of acid phosphatases with naphthol AS-phosphatases. *J. Natl. Cancer Inst.*, 21 : 523-539.
5) Curtiss, P. H. 1964. Changes produced in the synovial membrane and synovial fluid by disease. *J. Bone Joint Surg.*, 46-A : 873-888.
6) Cutlip, R. C. and Cheville, N. F. 1973. Structure of synovial membrane of sheep. *Amer. J. Vet. Res.*, 34 : 45-50.
7) Date, K. 1979. Scanning electron microscope studies on the synovial membrane. *Arch. Histol. Jpn.*, 42 : 517-531.
8) Delio, A. N., Sgambati, E., Brizzi, E., Pacini, P., Pacini, S., Ruggiero, M. and Gulisano, M. 1999. Distribution and characteristics of synoviocytes in the rabbit knee joint : a scanning/transmission electron microscopic study. *Ital. J. Anat. Embryol.*, 104 : 33-45.
9) Edwards, J. C. W. 1994. The nature and origins of synovium : experimental approaches to the study of synoviocyte differentiation. *J. Anat.*, 184 : 493-501.
10) Getty, R. 1975. *Sisson and Grossman's The Anatomy of Domestic Animals*, 5 th ed., pp. 42-44, Getty, R. ed., W. B. Saunders, Philadelphia.
11) Graabaek, P. M. 1982. Ultrastructural evidence for two distinct types of synoviocytes in rat synovial membrane. *J. Ultrastr. Res.*, 78 : 321-339.
12) Graabaek, P. M. 1984. Characteristics of the two types of synoviocytes in rat synovial membrane. An ultrastructural study. *Lab. Invest.*, 50 : 690-702.
13) Graabaek, P. M. 1985. Absorption of intraarticularly injected horseradish peroxidase in synoviocytes of rat synovial membrane : an ultrastructural cytochemical study. *J. Ultrastr. Res.*, 92 : 86-100.
14) Hago, B. E. D., Plummer, J. M. and Vaughan, L. C. 1990. Equine synovial tendon sheaths and bursae : an histological and scanning electron microscopical study. *Equine Vet. J.*, 22 : 264-272.
15) Iwanaga, T., Shikichi, M., Kitamura, H., Yanase, H. and Nozawa-Inoue, K. 2000. Morphology and functional roles of synoviocytes in the joint. *Arch. Histol. Cytol.*, 63 : 17-31.
16) Johansson, H.-E. and Rejno, S. 1976. Light and electron microscopic investigation of equine synovial membrane. *Acta Vet. Scand.*, 17 : 153-168.
17) Key, J. A. 1926. The mechanisms in-

volved in the removal of colloidal and particulate carbon from joint cavities. *J. Bone Joint Surg.*, 24 : 666-683.

18) Key, J. A. 1932. The synovial membrane of joints and bursae. In : *Special Cytology,* Vol. 1., pp. 753-766, Cowdry, E. V. ed., Paul B Hoeber Inc., New York.

19) Kitamura, H. P., Yanase, H., Kitamura, H. and Iwanaga, T. 1999. Unique localization of protein gene product 9.5 in type B synoviocytes in the joints of the horse. *J. Histochem. Cytochem.*, 47 : 343-351.

20) Krey, P. R. and Cohen, A. S. 1973. Fine structural analysis of rabbit synovial lining cells. I. The normal synovium and changes in organ culture. *Arth. Rheum.*, 16 : 324-340.

21) Lever, J. A. and Ford, E. H. R. 1958. Histological, histochemical and electron microscopic observations on synovial membrane. *Anat. Rec.*, 132 : 525-539.

22) Linck, G. and Porte, A. 1981. B-cells of the synovial membrane. IV. Ultrastructural evidence of secretory variations in hypophysectomized or propylthiouracyl -treated mice. *Cell Tissue Res.*, 218 : 123-128.

23) Mapp, P. I. and Revel, P. A. 1985. Fibronectine production by synovial intimal cells. *Rheumatol. Int.*, 5 : 229-237.

24) Matsubara, T., Spycher, M. A., Ruttner, J. R. and Fehr, K. 1983. The ultrastructural localization of fibronectin in the lining layer of the rheumatoid synovium : the synthesis of fibronectin by type B lining cells. *Rheumatol. Int.*, 3 : 75-79.

25) McDonald, J. N. and Levick, J. R. 1988. Morphology of surface synoviocytes in situ at normal and raised joint pressure, studied by scanning electron microscopy. *Ann. Rheum. Dis.*, 47 : 232-240.

26) Murakami, T. 1974. A revised tannin-osmium method for non-coated scanning electron microscope specimens. *Arch. Histol. Jpn.*, 36 : 189-193.

27) Naito, M., Hayashi, S., Yoshida, H., Nishikawa, S., Shuetz, L. D. and Takahashi, K. 1991. Abnormal differentiation of tissue macrophage populations in osteopetrosis (*op*) mice defective in the production of macrophage colony-stimulating factor. *Amer. J. Pathol.*, 139 : 657-667.

28) Nilsson, G. and Olsson, S. E. 1973. Radiologic and patho-anatomical changes in the distal joints and phalanges of the standardbred horse. *Acta Vet. Scand., Supplement*, 44 : 1-57.

29) Nio, J., Yokoyama, A., Okumura, M. and Iwanaga, T. 2002. Three-dimensional ultrastructure of synoviocytes in the knee joint of rabbits and morphological changes in osteoarthritis model. *Arch. Histol. Cytol.*, 65 : 189-200.

30) Okada, Y., Nakanishi, I. and Kajikawa, K. 1981. Ultrastructure of the mouse synovial membrane. Development and organization of the extracellular matrix. *Arth. Rheum.*, 24 : 838-843.

31) Roy, S. and Ghadially, F. N. 1967. Ultrastructure of normal rat synovial membrane. *Ann. Rheum. Dis.*, 26 : 26-38.

32) Roy, S. and Ghadially, F. N. 1967. Sythesis of hyaluronic acid by synovial cells. *J. Pathol. Bact.*, 93 : 555-557.

33) Senda, H., Sakuma, E., Wada, I., Wang, H. J., Maruyama, H. and Matsui, N. 1999. Ultrastructural study of cells at the synovium-cartilage junction : response of synovial cells of the rat knee joint to intra-articularly injected latex paticles. *Acta Anat. Nippon.*, 74 : 525-535.

34) Shannon, S. L. and Graham, R. C. 1971. Protein uptake by synovial cells. I. Ultrastructural study of the fate of intraarticularly injected peroxidases. *J. Histochem. Cytochem.*, 19 : 29-42.
35) Shikichi, M., Kitamura, H. P., Yanase, H., Konno, A., Takahashi-Iwanaga, H. and Iwanaga, T. 1999. Three-dimensional ultrastructure of synoviocytes in the horse joint as revealed by the scanning electron microscope. *Arch. Histol. Cytol.*, 62 : 219-229.
36) Shively, J. A. and Van Sickle, D. C. 1977. Scanning electron microscopy of equine synovial membrane. *Amer. J. Vet. Res.*, 38 : 681-684.
37) Southwick, W. O. and Bensch, K. G. 1971. Phagocytosis of colloidal gold by cells of synovial membrane. *J. Bone Joint Surg.*, 53-A : 729-741.
38) Steinberg, P. J. and Hodde, K. C. 1990. The morphology of synovial lining of various structures in several species as observed with scanning electron microscopy. *Scanning Microsc.*, 4 : 987-1020.
39) Takahashi-Iwanaga, H. and Fujita, T. 1986. Application of an NaOH maceration method to a scanning electron microscopic observation of Ito cells in the rat liver. *Arch. Histol. Jpn.*, 49 : 349-357.
40) Updike, S. J. and Diesen, C. D. 1983. Histologic appearance and distribution of synovial membrane types in the equine stifle joint. *Zent. Vet. C. Anat. Histol. Embryol.*, 12 : 53-59.
41) Woodward, D. H., Gryfe, A. and Gardner, D. L. 1969. Comparative study by scanning electron microscopy of synovial surfaces of four mammalian species. *Experientia*, 25 : 1301-1303.
42) Wysocki, G. P. and Brinkhous, K. M. 1972. Scanning electron microscopy of synovial membranes. *Arch. Pathol.*, 93 : 172-177.
43) Yielding, K. L., Tomkins, G. M. and Bunim, J. J. 1957. Synthesis of hyaluronic acid by human synovial tissue slices. *Science*, 125 : 1300.